International Journal of Control, Automation and Systems 19(1) (2021) 350-362
http://dx.doi.org/10.1007/s12555-019-0906-7
ISSN:1598-6446 eISSN:2005-4092
http://www.springer.com/12555

Fault Detection for a Class of Closed-loop Hypersonic Vehicle System via Hypothesis Test Method

Xunhong Lv, Yifan Fang, Zehui Mao, Bin Jiang*, and Ruiyun Qi

Abstract: This paper studies the fault detection problem for a class of hypersonic vehicle with actuator faults, disturbances and random noises. To handle the unknown disturbances, an unknown input Kalman filter (UIKF) is presented to estimate the unknown system states and disturbances, simultaneously. Considering that the closed-loop structure brings the robustness to the hypersonic vehicle, which could cover some faults, the Total Measurable Fault Information Residual (ToMFIR) is employed as the fault detection residual. Moreover, to deal with the random noises, the hypothesis testing method is utilized to obtain the thresholds under some fault detection performances (false alarm rate and missing alarm rate). The fault detectability condition is also derived. Finally, the simulations verify the effectiveness of the proposed fault detection method.

Keywords: Closed-loop system, fault detection, hypersonic vehicle, unknown input Kalman filter.

1. INTRODUCTION

Currently, hypersonic vehicles are widely used in military and civilian fields. The hypersonic vehicle has the characteristics of fast flight speed, strong penetration ability and large payload. The requirement for the safety and reliability of the hypersonic vehicle is very strict because of the particularity of the flight mission and the complexity of the flight environment [1]. There are many methods developed to maintain the stability of hypersonic vehicles, such as PID control method [2, 3], adaptive control [4]-[6], fuzzy control [7], back-stepping control [8], sliding mode control [9], and predictive control [10]. These control methods are mainly designed for fault-free systems. If faults occur in sensors, actuators or airframes, the hypersonic vehicle may be crashed. Fault detection and fault-tolerant control can increase the reliabilities of hypersonic vehicle systems. If faults could be detected timely and handled properly, the flight safety of the hypersonic vehicle can be ensured.

There also exist many literatures for systems with fault such as [11–16]. However, few closed-loop fault detection methods for hypersonic vehicle have been developed. In [17], the sliding-mode observer is used based on T-S fuzzy model for hypersonic vehicle to generate the residual and detect the fault in the actuator. In [18], weighted tube-based model predictive control combined with multi-purpose Luenberger state observer is applied to achieve passive fault accommodation. In [19], an active fault-tolerant control method using the information from adaptive observer is introduced via T-S fuzzy model. In [20], an observer method based on linear parameter-varying model is proposed to deal with multi-objective fault detection and isolation in the system with disturbances. These methods use the commands of actuators and outputs of sensors as indication signals for fault detection, and the original systems are seen as equivalent-open-loop systems. The equivalent-open-loop fault detection method ignores the improving robustness of closed-loop system. The operating characteristic of the open-loop system is changed and the robustness is enhanced while the closed-loop control law is introduced. It makes the system insensitive to external disturbances and some faults, that is, it has a certain ability of fault tolerance. If an equivalent-open-loop fault detection method is applied to a closed-loop system, it may work abnormally or its performance may be degraded.

Furthermore, disturbance and noise are unavoidable in hypersonic vehicle systems, and both contribute to the fault detection residuals. In existing literatures such as

Manuscript received November 1, 2019; revised March 30, 2020; accepted April 22, 2020. Recommended by Associate Editor Jiuxiang Dong under the direction of Editor Guang-Hong Yang. This work is supported by National Nature Science Foundation of China under Grant 61922042, 61773201, 61773201, and 61673207, the 111 project (B20007), Qing Lan Project, in part by the Fundamental Research Funds for the Central Universities under Grant NC2020002, NP2020103, and in part by National Key Laboratory of Science and Technology on Helicopter Transmission (Nanjing University of Aeronautics and Astronautics) under Grant HTL-O-19G11.

Xunhong Lv, Yifan Fang, Zehui Mao, Bin Jiang, and Ruiyun Qi are with the College of Automation Engineering, Nanjing University of Aeronautics and Astronautics (NUAA), Nanjing 210016, China (e-mails: lvxh@nuaa.edu.cn, 15850631768@163.com, zehuimao@nuaa.edu.cn, binjiang@nuaa.edu.cn, ruiyun.qi@nuaa.edu.cn). Bin Jiang is also with National Key Laboratory of Science and Technology on Helicopter Transmission, NUAA, China.
* Corresponding author.

[21, 22], robust residuals are obtained under the precondition that the uncertainty has an upper bound, and thresholds with certain disturbance rejection capacity are chosen. However, it is difficult to obtain the upper bound of the statistical noise in general. In addition, many robust fault detection methods like [23–25] are developed with considering only one of the bounded disturbance and random noise, but they exist simultaneously in fact.

Finally, the quantitative analysis of the fault detection algorithms is rarely considered in the existing results, and performance indicators such as missing alarm rate and false alarm rate are ignored.

In this paper, a closed-loop fault detection method is developed for hypersonic vehicle systems in the presence of the actuator faults, disturbances and random noise, and the missing alarm rate and false alarm rate of the detection are also provided.

The major contributions of this paper are summarized as follows:

1) For the hypersonic vehicle system with the actuator faults, the disturbance and random noise are taken into consideration under the closed-loop structure. To deal with the disturbance and faults simultaneously, an unknown input Kalman filter (UIKF) is presented to estimate the unmeasured states and disturbances.
2) Based on the estimated states and disturbances, the Total Measurable Fault Information Residual (ToMFIR) method is employed to generate the fault detection residual under the closed-loop control. Using the hypothesis testing, the fault detection scheme is derived with the false and missing alarm rate performance and fault detectability condition.

Remark 1: The contributions of this paper have some advantages compared with other methods. The comparisons of the methods proposed in this paper and the published alternatives are show as follows: 1) The traditional Kalman filter can only handle the system without the presence of unknown inputs, yet UIKF can deal with the unknown inputs in the hypersonic vehicle system. 2) In the closed-loop system, the equivalent-open-loop residual is insensitive to some faults. However, ToMFIR contains both the controller residual information and the output residual information, which makes the ToMFIR work out well in the closed-loop hypersonic vehicle system. 3) Simple threshold judgement method does not work well in the presence of random noises. Hypothesis test method not only can deal with random noises, but also gives the false alarm rate and missing alarm rate of the fault detection.

The rest of this paper is organized as follows: In Section 2, the dynamical model of closed-loop hypersonic vehicle systems with actuator faults, disturbance and random noise is presented. In Section 3, an UIKF is developed for the faulty-free case to estimate the unmeasured states and disturbances, and the residual is generated using the ToMFIR method. In Section 4, the fault detection scheme is proposed with the fault detectability condition. In Section 5, simulations for healthy and faulty cases are presented. Finally, Section 6 concludes the paper.

2. SYSTEM DESCRIPTION AND PROBLEM STATEMENT

Consider the hypersonic vehicle (see [26, 27]), whose continuous-time longitudinal state-model is described as

$$\dot{x}(t) = A'x(t) + B'u(t) + D'd(t) + n_1'(t), \tag{1}$$
$$y(t) = C'x(t) + n_2'(t), \tag{2}$$

where the state vector $x = [V,\ \alpha,\ q,\ \theta,\ h]^T \in R^5$ consists of speed V, angle of attack α, pitch rate q, pitch angle θ and altitude h, the output vectors $y = [V_m,\ \alpha_m,\ q_m,\ \theta_m,\ h_m]^T \in R^5$ consists of measurements of the state vectors, and the input signals $u = [\delta_e,\ \eta]^T \in R^2$ are elevator deflection and throttle setting. $d(t) = [V_W,\ \alpha_W]^T \in R^2$ is the wind field disturbance with its distribution matrix $D' \in R^{5\times 2}$ (see [28] and [29]). The process noise $n_1'(t) \in R^5$ and sensor noise $n_2'(t) \in R^5$ are considered, which both independently subject to Gaussian distribution, provided with zero means and covariance matrix $Q'(t) = diag\{q_1'^2(t),\ q_2'^2(t),\ \cdots,\ q_5'^2(t)\}$, $R'(t) = diag\{r_1'^2(t),\ r_2'^2(t),\ \cdots,\ r_5'^2(t)\}$. A', B', C' are the system matrices with appropriate dimensions linearized from the general hypersonic vehicle $\dot{x} = f(x,u)$ (see [26, 27]), which are expressed as

$$A' = \frac{\partial f(x,u)}{\partial x}|_{x=x_0,u=u_0} \in R^{5\times 5}, \tag{3}$$
$$B' = \frac{\partial f(x,u)}{\partial u}|_{x=x_0,u=u_0} \in R^{5\times 2}, \tag{4}$$
$$C' = \begin{bmatrix} 1 & 0 & 0 & 0 & 0 \\ 0 & 1 & 0 & 0 & 0 \\ 0 & 0 & 1 & 0 & 0 \\ 0 & 0 & 0 & 1 & 0 \\ 0 & 0 & 0 & 0 & 1 \end{bmatrix} \in R^{5\times 5}, \tag{5}$$
$$f(x,u) = \begin{bmatrix} \frac{T(V,\eta)\cos\alpha - R(V,\alpha)}{m} - g(h)\sin(\theta-\alpha) \\ q - \frac{L(V,\alpha)+T(V,\eta)\sin\alpha}{mV} + \frac{g(h)\cos(\theta-\alpha)}{V} \\ M(V,\alpha,q,\delta_e)/I_{yy} \\ q \\ V\sin(\theta-\alpha) \end{bmatrix}, \tag{6}$$

with x_0, u_0 being the trim point under the cruise phase, T, L and R being thrust, lift and drag forces, M being the pitching moment, and I_{yy} being the moment of inertia.

Similar to the fixed-wing plane, the actuators of the hypersonic vehicle are elevator and throttle, for which the faults, such as lock in place, float, hard over fault, loss of effectiveness, etc., could occur, which result in the performance degradation. Considering the actuator faults, the input signal of the hypersonic vehicle model (1) can be rewritten as

$$u(t) = v(t) + f(t), \tag{7}$$

where $v(t)$ is the designed control signal, and the unknown vector field $f(t) \in R^2$ represents the deviation in the actuator due to a fault. It can be seen as a loss-of-effectiveness fault, the input signal is expressed:

$$u(t) = v(t) + (I - \Lambda)v(t), \tag{8}$$

where $\Lambda \in R^2$ is a diagonal matrix with its elements belonging to $[0, 1)$. As we set $f(t) = (I - \Lambda)v(t)$, (8) is equivalent to (7). For the lock-in-place fault, the input signal is expressed:

$$u(t) = u_c, \tag{9}$$

where u_c is a constant representing the place that the actuator locks. As we rewrite (8) as $u(t) = v(t) + (u_c - v(t))$, and set $f(t) = u_c - v(t)$, (8) can also be equivalent to (7). From now on, we can see that the fault model (7) can represent a lot of actuator faults of the hypersonic vehicle.

Considering that the flight control computer which is introduced into the aircraft control system is discrete-time in practice, the discrete-time fault detection scheme should be induced, which is more practical and has the potential application in the real flight control system. Therefore, under the sampling time T, the hypersonic vehicle model (1)-(7) can be discretized as

$$x(k+1) = Ax(k) + Bv(k) + Dd(k) + F_a f(k) + n_1(k), \tag{10}$$

$$y(k) = Cx(k) + n_2(k), \tag{11}$$

where $A = e^{A'T}$, $B = \int e^{A'T} B' d\tau$, $C = C'$, $D = \int e^{A'T} D' d\tau$, $F_a = B$, $n_1(k) = \int e^{A'T} d\tau n_1{}'(k)$ with its the covariance matrix $Q(k) = diag\{q_1{}^2(k), q_2{}^2(k), \cdots, q_5{}^2(k)\}$, and $n_2(k) = n_2'(k)$ with its covariance matrix $R(k) = diag\{r_1{}^2(k), r_2{}^2(k), \cdots, r_5{}^2(k)\}$. From now on, the mathematical model for the hypersonic vehicle with actuator faults is established as (10)-(11), for which we will force on the fault detection problem.

Further, to guarantee the hypersonic vehicle system (10)-(11) stable, a controller $v(t)$ should be designed. In this paper, the state feedback controller is used:

$$v(k) = -Kx(k), \tag{12}$$

where K is the appropriate feedback gain matrix to ensure the hypersonic vehicle system (10)-(11) stable, even have some robust performance for some disturbances.

It should be pointed out that the hypersonic vehicle model (10)-(11) with the controller (12) is a closed-loop system, which induces the fault detection problem more complex than that of the open-loop system. The difficulty of fault detection for closed-loop structure, is that the controller could handle some faults to eliminate the deviations, which often be reflected in the output signal. The conventional fault detection method, which is constructed by the actuator output and system output, could be invalid for the closed-loop system. Thus, the researching on the fault detection under the closed-loop structure is meaningful.

Remark 2: Although the state feedback controller is simple and easily-realized, but it also has the robustness for some disturbances, which means the controller $v(k)$ in (12) can be considered as a passive fault-tolerant controller for some faults. Thus, the hypersonic vehicle (10)-(11) with the controller (12) can mainly display the fault detection problem for the closed-loop control system.

Remark 3: It is obvious that the hypersonic vehicle model (10)-(11) has disturbances and stochastic noises, which requires a robust controller. Moreover, the disturbances and stochastic noises could cause the states (also the outputs) deviate their normal values, which leads to the alarms in the fault detection. To deal with the disturbances, stochastic noises and faults, simultaneously, the robust fault detection filter will be proposed in this paper.

The objective of this paper can be summarized as to design a filter-based actuator fault detection scheme for the hypersonic vehicle model (10)-(12) with unknown external process and sensor noises under the closed-loop structure. The key technology is to figure out a residual generation method and choose appropriate thresholds to detect the faults effectively.

3. FAULT DETECTION

There are many methods for fault detection, and filter-based fault detection is a hot spot. Filter-based fault detection methods mainly include residual-based fault detection and fault estimation-based fault detection. The fault detection method applied herein is residual-based fault detection, and the residual is generated by using the available information in the monitored system to determine whether the fault occurs. In this section, an unknown input Kalman filter will be proposed to obtain the residual.

3.1. Fault detection Kalman filter

The traditional Kalman filters can only handle the system without the presence of unknown inputs. To deal with the unknown wind field disturbance in the system (10)-(12), an unknown input Kalman filter (UIKF) is adopted to estimate the system states and disturbances simultaneously. For the fault detection filter design, the following assumption will be used.

Assumption 1 [30]**:** The matrix D is full rank, i.e., $rank(D) = q$.

According to [31] and [32], the minimum-variance unbiased UIKF is designed for (10)-(12) as

$$\hat{x}(k+1/k)=\bar{A}\hat{x}(k/k), \tag{13}$$

$$P(k+1/k)=\bar{A}P(k/k)\bar{A}^T+Q, \tag{14}$$

$$\begin{aligned}&\hat{x}(k+1/k+1)\\&=\hat{x}(k+1/k)+L^x(k+1)\left[y(k+1)-C\left(\hat{x}(k+1/k)\right)\right],\end{aligned} \tag{15}$$

$$\hat{d}(k+1/k)=L^d(k+1)\left[y(k+1)-C\hat{x}(k+1/k)\right], \tag{16}$$

$$\begin{aligned}&P(k+1/k+1)\\&=P(k+1/k)-P(k+1/k)C^T\Delta^{-1}(k+1)CP(k+1/k)\\&\quad+\Lambda(k+1)D^TC^T\Delta^{-1}(k+1)CD\Lambda^T(k+1),\end{aligned} \tag{17}$$

$$P^d(k+1/k)=\left(D^TC^T\Delta^{-1}CD\right)^{-1}, \tag{18}$$

where $\bar{A}=A-BK$, $\hat{x}(k+1/k)$ is the predicted value of $x(k+1)$ with its variance matrix $P(k+1/k)$, $\hat{x}(k+1/k+1)$ is the estimation of $x(k+1)$ with its variance matrix $P(k+1/k+1)$, $\hat{d}(k+1/k)$ is the estimation of $d(k)$ with its variance matrix $P^d(k+1/k)$, Q and R are the known variance matrices of the noises $n_1(k)$ and $n_2(k)$, respectively. The parameter matrices $L^x(k+1)$, $L^d(k+1)$, $\Delta(k+1)$, and $\Lambda(k+1)$ are designed as

$$\begin{aligned}L^x(k+1)&=P(k+1/k)C^T\Delta^{-1}(k+1)\\&\quad+\Lambda(k+1)D^TC^T\Delta^{-1}(k+1),\end{aligned} \tag{19}$$

$$L^d(k+1)=(D^TD)^{-1}D^TL^x(k+1), \tag{20}$$

$$\Delta(k+1)=CP(k+1/k)C^T+R, \tag{21}$$

$$\begin{aligned}\Lambda(k+1)&=\left[D-P(k+1/k)C^T\Delta^{-1}(k+1)CD\right]\\&\quad\times\left[D^TC^T\Delta^{-1}(k+1)CD\right]^{-1}.\end{aligned} \tag{22}$$

Denote the estimation errors $e(k+1)=x(k+1)-\hat{x}(k+1/k+1)$ and $e_d(k)=d(k)-\hat{d}(k+1/k)$. For the faulty-free case (i.e., $f(k)=0$ in (10)-(12)), it has the error $e(k+1)$ expressed as

$$\begin{aligned}e(k+1)=&x(k+1)-\hat{x}(k+1/k+1)\\=&x(k+1)-\hat{x}(k+1/k)\\&-L^x(k+1)\big(Cx(k+1)+n_2(k+1)\\&-C\hat{x}(k+1/k)\big)\\=&\left(I-L^x(k+1)C\right)\left(x(k+1)-\hat{x}(k+1/k)\right)\\&-L^x(k+1)n_2(k+1)\\=&\left(I-L^x(k+1)C\right)\left(\bar{A}e(k)+Dd(k)+n_1(k)\right)\\&-L^x(k+1)n_2(k+1).\end{aligned} \tag{23}$$

Moreover, if and only if $\operatorname{rank}(CD)=\operatorname{rank}(D)=q$, substituting (22) into (19) gives

$$\begin{aligned}&L^x(k+1)CD\\&=P(k+1/k)C^T\Delta^{-1}(k+1)CD\\&\quad+\left[D-P(k+1/k)C^T\Delta^{-1}(k+1)CD\right]\\&\quad\times\left[D^TC^T\Delta^{-1}(k+1)CD\right]^{-1}D^TC^T\Delta^{-1}(k+1)CD\\&=P(k+1/k)C^T\Delta^{-1}(k+1)CD\\&\quad+\left[D-P(k+1/k)C^T\Delta^{-1}(k+1)CD\right]\\&=D,\end{aligned} \tag{24}$$

where $\operatorname{rank}(CD)=\operatorname{rank}(D)=q$ holds if Assumption 1 is satisfied (see [30]).

Due to the zero-mean noises n_1 and n_2, and using (24), the mean of (23) can be calculated

$$\begin{aligned}\mathrm{E}\{e(k+1)\}&=\left(\bar{A}-L^x(k+1)C\bar{A}\right)\mathrm{E}\{e(k)\}\\&\quad+\left(D-L^x(k+1)CD\right)\mathrm{E}\{d(k)\}\\&=\left(\bar{A}-L^x(k+1)C\bar{A}\right)\mathrm{E}\{e(k)\}.\end{aligned} \tag{25}$$

Further, according to [33] and [34], if $\hat{x}(0/0)=\mathrm{E}\{x(0)\}$ for (25), then

$$\begin{aligned}&\mathrm{E}\{e(k+1)\}\\&=\left(\bar{A}-L^x(k+1)C\bar{A}\right)\mathrm{E}\{e(k)\}\\&=\left(\bar{A}-L^x(k+1)C\bar{A}\right)\cdots\left(\bar{A}-L^x(1)C\bar{A}\right)\mathrm{E}\{e(0)\}\\&=\left(\bar{A}-L^x(k+1)C\bar{A}\right)\cdots\left(\bar{A}-L^x(1)C\bar{A}\right)\\&\quad\times\mathrm{E}\{x(0)-\hat{x}(0/0)\}\\&=0.\end{aligned} \tag{26}$$

Similarly, we can obtain

$$\begin{aligned}&\mathrm{E}\{e_d(k)\}\\&=\mathrm{E}\left\{d(k)-\hat{d}(k+1/k)\right\}\\&=\mathrm{E}\left\{d(k)-L^d(k+1)\left(y(k+1)-C\hat{x}(k+1/k)\right)\right\}\\&=\mathrm{E}\left\{d(k)-L^d(k+1)\left(C\bar{A}e(k)+CDd(k)\right)\right\}\\&=\mathrm{E}\left\{d(k)-(D^TD)^{-1}D^TL^x(k+1)CDd(k)\right\}\\&\quad+\mathrm{E}\left\{-L^d(k+1)C\bar{A}e(k)\right\}\\&=\mathrm{E}\left\{-L^d(k+1)C\bar{A}e(k)\right\}\\&=0.\end{aligned} \tag{27}$$

Based on (26) and (27), we can conclude that $\hat{x}(k/k)$ and $\hat{d}(k+1/k)$ are the indeed unbiased estimators of $x(k)$ and $d(k)$. From the above analysis, we can obtain the existence condition of the UIKF (13)-(18) and summarize the following theorem.

Theorem 1: Consider the hypersonic vehicle system (10)-(12) under the faulty-free case (i.e., $f(k)=0$) and Assumption 1, the unknown input Kalman filter (UIKF) (13)-(18) is an unbiased estimator.

Discussion: As stated in [26, 27], under the trimmed point $[x_0, v_0]=[8930, 0.1, 0, 0.1, 85700, 0, 0]$, the matrices A', B' in the system (1)-(2) can be calculated by (3)-(4) as

$$A'=\begin{bmatrix}a_{11}&a_{12}&0&a_{14}&a_{15}\\a_{21}&a_{22}&a_{23}&a_{24}&a_{25}\\a_{31}&a_{32}&a_{33}&0&0\\0&0&a_{43}&0&0\\a_{51}&a_{52}&0&a_{54}&0\end{bmatrix},\quad B'=\begin{bmatrix}0&b_{12}\\0&b_{22}\\b_{31}&0\\0&0\\0&0\end{bmatrix},$$

where

$$\begin{cases}
a_{11}=\frac{\rho VS}{m}\left[\left(C_T^{\eta}\eta+C_T^0\right)\cos\alpha-\left(C_D^{\alpha^2}\alpha^2+C_D^{\alpha}\alpha+C_D^0\right)\right],\\
a_{12}=\frac{\rho V^2S}{2m}\left[-\left(C_T^{\eta}\eta+C_T^0\right)\sin\alpha-\left(2C_D^{\alpha^2}\alpha+C_D^{\alpha}\right)\right]\\
\qquad +\frac{\mu}{r^2}\cos\left(\theta-\alpha\right),\\
a_{14}=-\frac{\mu}{r^2},\\
a_{15}=-\frac{2\mu}{r^3}\sin\left(\theta-\alpha\right),\\
a_{21}=-\frac{\rho S}{2m}\left[\left(C_T^{\eta}\eta+C_T^0\right)+\left(C_L^{\alpha}\alpha+C_L^0\right)\right]\\
\qquad -\frac{\mu}{V^2r^2}\sin\left(\theta-\alpha\right),\\
a_{22}=-\frac{\rho VS}{2m}C_L^{\alpha}-\frac{\mu}{Vr^2}\cos\left(\theta-\alpha\right),\\
a_{23}=1,\\
a_{24}=\frac{\mu}{Vr^2}\cos\left(\theta-\alpha\right),\\
a_{25}=-\frac{2\mu}{Vr^3}\sin\left(\theta-\alpha\right),\\
a_{31}=\frac{\rho VS\bar{c}}{I_{yy}}\left[\left(C_M^{\alpha^2}\alpha^2+C_M^{\alpha}\alpha+C_M^0\right)+c_e\left(\delta_e-\alpha\right)\right]\\
\qquad +\frac{\rho S\bar{c}^2q}{4I_{yy}}\left(C_M^{\alpha^2q}\alpha^2+C_M^{\alpha q}\alpha+C_M^{q0}\right),\\
a_{32}=\frac{\rho V^2S\bar{c}}{2I_{yy}}\left[\left(2C_M^{\alpha^2}\alpha+C_M^{\alpha}\right)\right.\\
\qquad \left.+\frac{\bar{c}q}{2V}\left(2C_M^{\alpha^2q}\alpha+C_M^{\alpha q}\right)-c_e\right],\\
a_{33}=\frac{\rho V^2S\bar{c}}{2I_{yy}}\left[\frac{\bar{c}}{2V}\left(C_M^{\alpha^2q}\alpha^2+C_M^{\alpha q}\alpha+C_M^{q0}\right)\right],\\
a_{43}=1,\\
a_{51}=V\sin\left(\theta-\alpha\right),\\
a_{52}=-V\cos\left(\theta-\alpha\right),\\
a_{54}=V\cos\left(\theta-\alpha\right),\\
r=h+R_E,\\
b_{12}=\frac{\rho V^2S}{2m}C_T^{\eta}\cos\alpha,\\
b_{22}=-\frac{\rho VS}{2m}C_T^{\eta},\\
b_{31}=\frac{\rho V^2S\bar{c}}{2I_{yy}}c_e,
\end{cases}$$

the values of the parameters are shown in Table 1. According to $A=e^{A'T}$,$B=\int e^{A'T}B'd\tau$, $C=C'$, $D=\int e^{A'T}D'd\tau$, and with the sampling time $T=0.01s$, the matrices A, B, C, D, in the system (10)-(12) can be obtained as

$$A=\begin{bmatrix}1.000 & 7.8008\times10^{-1} & 2.3227\times10^{-3} & -3.1550\times10^{-1} & 0\\ -2.7215\times10^{-9} & 9.9971\times10^{-1} & 9.9963\times10^{-3} & 3.5328\times10^{-5} & 0\\ 3.5507\times10^{-8} & 1.6649\times10^{-4} & 9.9952\times10^{-1} & 2.6604\times10^{-9} & 0\\ 1.7755\times10^{-10} & 8.3253\times10^{-7} & 9.9976\times10^{-3} & 1.0000 & 0\\ 1.2945\times10^{-7} & -8.9287\times10^{1} & 3.8529\times10^{-5} & 8.9298\times10^{1} & 1.000\end{bmatrix},$$

Table 1. Hypersonic vehicle parameters (see in [27]).

Symbol	Description	Value	unit
S	Reference area	3603	ft^2
m	Mass	9375	slug
μ	Gravitational constant	1.39×10^{16}	$\mathrm{ft}^3\cdot\mathrm{s}^{-2}$
I_{yy}	Moment of inertia	7×10^{6}	$\mathrm{slug}\cdot\mathrm{ft}^2$
R_E	Radius of Earth	20903500	ft
ρ	Density of air	0.24325×10^{-4}	$\mathrm{slug}\cdot\mathrm{ft}^{-3}$
$\bar{c}$	Mean aerodynamic chord	80	ft
c_e	Constant	0.0292	
C_T^{η}	Coefficient	$\begin{cases}0.02576, \eta\leqslant1\\0.00336, \eta>1\end{cases}$	rad^{-1}
C_T^{0}	Coefficient	$\begin{cases}0, \eta\leqslant1\\0.02240, \eta>1\end{cases}$	
C_L^{α}	Coefficient	0.6203	rad^{-1}
C_L^{0}	Coefficient	0	
$C_D^{\alpha^2}$	Coefficient	−0.6450	rad^{-2}
C_D^{α}	Coefficient	0.0043378	rad^{-1}
C_D^{0}	Coefficient	0.003772	
$C_M^{\alpha^2}$	Coefficient	−0.035	rad^{-2}
C_M^{α}	Coefficient	0.036617	rad^{-1}
C_M^{0}	Coefficient	5.361×10^{-6}	
$C_M^{\alpha^2q}$	Coefficient	−6.796	$\mathrm{s}\cdot\mathrm{rad}^{-3}$
$C_M^{\alpha q}$	Coefficient	0.3015	$\mathrm{s}\cdot\mathrm{rad}^{-2}$
C_M^{q0}	Coefficient	−0.2289	$\mathrm{s}\cdot\mathrm{rad}^{-1}$

$$B=\begin{bmatrix}9.0296\times10^{-6} & 9.5537\times10^{-2}\\ 5.8295\times10^{-5} & -1.0751\times10^{-5}\\ 1.1659\times10^{-2} & 8.0113\times10^{-10}\\ 5.8300\times10^{-5} & 2.6710\times10^{-12}\\ 1.1233\times10^{-7} & 4.8006\times10^{-4}\end{bmatrix},$$

$$C=\begin{bmatrix}1&0&0&0&0\\0&1&0&0&0\\0&0&1&0&0\\0&0&0&1&0\\0&0&0&0&1\end{bmatrix},$$

$$D=\begin{bmatrix}-3.6356\times10^{-5} & 1.0010\times10^{-2}\\ 4.9258\times10^{-7} & 9.6787\times10^{-4}\\ -2.0142\times10^{-5} & -3.0347\times10^{-2}\\ 1.0072\times10^{-7} & 1.5175\times10^{-4}\\ -1.7498\times10^{-5} & -3.6442\times10^{-2}\end{bmatrix},$$

and K is given as

$$K=\begin{bmatrix}1.5756 & 1.8829\times10^{2} & -4.2797 & 2.0884\times10^{2} & -2.2026\\ -1.0486 & 5.5725 & 0.1107 & -5.0335 & -0.0244\end{bmatrix}.$$

It can be checked that $\mathrm{rank}(CD)=\mathrm{rank}(D)=2$, which means Assumption 1 is satisfied and the unbiased UIKF (13)-(18) exists for the hypersonic vehicle.

3.2. ToMFIR (Total measurable fault information residual)

Based on the proposed Kalman filter (13)-(18), a residual can be generated for actuator fault detection of the hypersonic vehicle (10)-(12) under the closed-loop structure. The residual generator ToMFIR, which was first introduced in [35], will be used here. The ToMFIR is independent of the filter gains and contains the essential fault information:

$$\begin{aligned} r(k) =& G(k)v(k) - G_0(k)v(k) \\ =& G(k)v(k) - G_0(k)v_0(k) \\ & - (G_0(k)v(k) - G_0(k)v_0(k)) \\ =& r_y(k) - G_0(k)r_v(k), \end{aligned} \tag{28}$$

where $r_y(k) = y(k) - y_0(k)$ indicates the output residual, $r_v(k) = v(k) - v_0(k)$ indicates the controller residual and G_0 is the parallel plant. Equation (28) contains both the controller residual information and the output residual information, which makes the ToMFIR work out well in the closed-loop hypersonic vehicle system.

A parallel system G_0 is built up to compare with the original system (10)-(12) as

$$x_0(k+1) = Ax_0(k) + Bv_0(k) + D\hat{d}(k+1/k), \tag{29}$$

$$y_0(k) = Cx_0(k), \tag{30}$$

$$v_0(k) = -Kx_0(k), \tag{31}$$

where $x_0(k) \in R^5$ is the state, $y_0(k) \in R^5$ is the measurable output vector, $\hat{d}(k+1/k)$ is the estimate of $d(k)$, and $v_0(k) \in R^2$ is the input.

From (10)-(12)and (29)-(31), we can obtain

$$\begin{aligned} r_y(k) =& y(k) - y_0(k) \\ =& Cx(k) + n_2(k) - Cx_0(k) \\ =& C\Big[Ax(k-1) + Bv(k-1) + Dd(k-1) \\ & + F_a f(k-1) + n_1(k-1) - Ax_0(k-1) \\ & - Bv_0(k-1) - D\hat{d}(k/k-1)\Big] + n_2(k) \\ =& C\Big[A\left(x(k-1) - x_0(k-1)\right) \\ & + B\left(v(k-1) - v_0(k-1)\right) \\ & + Dr_d(k-1) + F_a f(k-1) + n_1(k-1)\Big] \\ & + n_2(k) \\ =& CA^k r_x(0) + C\sum_{n=0}^{k-1} A^{k-n-1} Dr_d(n) \\ & + C\sum_{n=0}^{k-1} A^{k-n-1} F_a f(n) + n_2(k) \\ & + C\sum_{n=0}^{k-1} A^{k-n-1} n_1(k) \\ & + C\left(Bv(k-1) - Bv_0(k-1)\right), \end{aligned} \tag{32}$$

where $r_x(k) = x(k) - x_0(k)$ and $r_d(k) = d(k) - \hat{d}(k+1/k)$.

Substituting (32) into (28), TOMFIR is in the form of

$$\begin{aligned} r(k) =& r_y(k) - G_0(k)r_v(k) \\ =& CA^k r_x(0) + C\sum_{n=0}^{k-1} A^{k-n-1} Dr_d(n) \\ & + C\sum_{n=0}^{k-1} A^{k-n-1} F_a f(n) + C\sum_{n=0}^{k-1} A^{k-n-1} n_1(k) \\ & + n_2(k) + C\left(Bv(k-1) - Bv_0(k-1)\right) \\ & - C\left(Bv(k-1) - Bv_0(k-1)\right) \\ =& CA^k r_x(0) + C\sum_{n=0}^{k-1} A^{k-n-1} Dr_d(n) \\ & + C\sum_{n=0}^{k-1} A^{k-n-1} F_a f(n) \\ & + C\sum_{n=0}^{k-1} A^{k-n-1} n_1(k) + n_2(k). \end{aligned} \tag{33}$$

In the most existing results, the robust residuals are obtained for the uncertainty with a upper bound. However, for the residual (33), there are the stochastic noises, whose upper bounds do not exist. Then, probabilistic method will be employed to determine the thresholds for fault detection.

4. THE ANALYSIS FOR FAULT DETECTION PERFORMANCE

In this section, the thresholds will be determined by using hypothesis test method to make decision and make the FD effective.

4.1. Residual evaluation

According to the UIKF (13)-(18) in Section 3, the distribution of $r_d(k)$ can be obtained as $r_d(k) \sim N\left(0, P^d(k+1/k)\right)$.

Based on the residual expression (33), and for the healthy case ($f(k) = 0$), it has

$$\begin{aligned} r(k) =& CA^k r_x(0) + C\sum_{n=0}^{k-1} A^{k-n-1} Dr_d(n) + n_2(k) \\ & + C\sum_{n=0}^{k-1} A^{k-n-1} n_1(k), \end{aligned} \tag{34}$$

where $r(k)$ subjects to Gaussian distribution, with its mean and variance take the form as

$$\mathrm{E}\{r(k)\} = CA^k r_x(0) = E_r(k),$$

$$
\begin{aligned}
&\mathrm{Var}\{r(k)\}\\
&=C\sum_{n=0}^{k-1}A^{k-n-1}DP^{d}(n+1/n)D^{T}(A^{k-n-1})^{T}C^{T}\\
&\quad+C\sum_{n=0}^{k-1}A^{k-n-1}Q(A^{k-n-1})^{T}C^{T}+R\\
&=V_r(k).
\end{aligned}
$$

Therefore, the distribution of the residual (34) is $r(k)\sim N(E_r(k),V_r(k))$.

Similarly, under the case that the actuator fault occurs ($f(k)\neq 0$), ToMFIR is rewritten as

$$
\begin{aligned}
r(k)=&CA^{k}r_x(0)+C\sum_{n=0}^{k-1}A^{k-n-1}Dr_d(n)+n_2(k)\\
&+C\sum_{n=0}^{k-1}A^{k-n-1}F_af(n)+C\sum_{n=0}^{k-1}A^{k-n-1}n_1(k),
\end{aligned}
\tag{35}
$$

which also subjects to Gaussian distribution, with its mean and variance take the form as

$$
\begin{aligned}
&\mathrm{E}\{r(k)\}=E_r(k)+C\sum_{n=0}^{k-1}A^{k-n-1}F_af(n),\\
&\mathrm{Var}\{r(k)\}=V_r(k).
\end{aligned}
$$

Therefore, the distribution of the residual (35) is $r(k)\sim N\big(E_r(k)+C\sum_{n=0}^{k-1}A^{k-n-1}F_af(n),V_r(k)\big)$.

According to residuals (34)-(35), it can be seen that the change of $\mathrm{E}\{r(k)\}$ suggests the occurrence of the actuator fault in the hypersonic vehicle. For fault detection, the following hypothesis testing is designed:

$$
H_0:\mathrm{E}\{r(k)\}=E_r(k),H_1:\mathrm{E}\{r(k)\}\neq E_r(k). \tag{36}
$$

Under healthy case, the acceptance region $X(k)$ of the hypothesis test is presumed to fulfill

$$
P(r(k)\in X(k)|H_0)=1-\lambda, \tag{37}
$$

where λ is a small positive scalar and determines the test size.

Then $X(k)$ is in the form as

$$
\begin{aligned}
X(k)&=[m(k),n(k)]\\
&=\Big[E_r(k)-h_{\lambda/2}\sqrt{\mathrm{Var}\{r(k)|H_0\}}\bar{E},\\
&\qquad E_r(k)+h_{\lambda/2}\sqrt{\mathrm{Var}\{r(k)|H_0\}}\bar{E}\Big],
\end{aligned}
\tag{38}
$$

where $\mathrm{Var}\{r(k)|H_0\}=V_r(k)$, $\bar{E}=\underbrace{[1,1,\dots1]}_{r}^{T}$ and $h_{\lambda/2}$ is a positive scalar which means that a variable subjecting to the standard normal distribution has the probability of λ in the interval $(-\infty,-h_{\lambda/2}]\cup[h_{\lambda/2},+\infty)$.

In summary, the actuator fault in the hypersonic vehicle system can be detected through the following rules. While $r(k)\notin X(k)$, there may be an actuator fault appearing in the system. The random variable $T_d<+\infty$ is defined as the time at which the fault is detected, and T_f is defined as the unknown moment at which the fault appears. It takes $T_d=inf\{k>T_f:r(k)\notin X(k)\}$. It should be noted that for the high reliable performance of the hypersonic vehicle, T_d-T_f should be as small as possible. Moreover, the false alarm rate can be given as

$$
P\left(D_{test}(k)=H_1|H_0\right)=1-P\left(r(k)\in X(k)|H_0\right)=\lambda, \tag{39}
$$

in which $D_{test}(k)$ implies the test decision at the moment k.

On the basis of the hypothesis test (36) and similar to the analysis of the healthy case, under the case that actuator fault appears ($k>T_f$) in the hypersonic vehicle, the acceptance region $Y(k)\in R^5$ for the faulty hypersonic vehicle is presumed to meet

$$
P\left(r(k)\in Y(k)|H_1\right)=1-\gamma,k>T_f, \tag{40}
$$

where γ is a small positive scalar and determines the test size.

Then, it takes

$$
\begin{aligned}
Y(k)&=[w(k),z(k)]\\
&=\Big[\mathrm{E}\{r(k)|H_1\}-h_{\gamma/2}\sqrt{\mathrm{Var}\{r(k)|H_1\}}\bar{E},\\
&\qquad \mathrm{E}\{r(k)|H_1\}+h_{\gamma/2}\sqrt{\mathrm{Var}\{r(k)|H_1\}}\bar{E}\Big],
\end{aligned}
\tag{41}
$$

wherein $\mathrm{E}\{r(k)|H_1\}=E_r(k)+C\sum_{n=0}^{k-1}A^{k-n-1}F_af(n)$, $\mathrm{Var}\{r(k)|H_1\}=V_r(k)$ and $h_{\gamma/2}$ is a positive scalar which means that a variable subjecting to the standard normal distribution has the probability of γ in the interval $(-\infty,-h_{\gamma/2}]\cup[h_{\gamma/2},+\infty)$.

Redefine the random variable $\hat{T}_d<+\infty$ as the time at which the actuator fault in the hypersonic vehicle system is detected. Therefore, if it satisfies that $\hat{T}_d<+\infty$, the actuator fault can be detected with $\hat{T}_d=inf\{k>T_f:X(k)\cap Y(k)=\varnothing\}$. Moreover, $\hat{T}_d-T_f$ should also be as small as possible for hypersonic vehicle to guarantee the safety performance.

4.2. Necessary conditions for fault detection

Intuitively, an actuator fault of a hypersonic vehicle is detectable if the mean estimate could exceed the test acceptance region at the time $\hat{T}_d<+\infty$. The condition of fault detectability can be derived.

Theorem 2: For an actuator fault $f(k)$ in the hypersonic vehicle system, a finite value $\hat{T}_d\geq T_f$ exists if and only if that the ith element of $f(k)$ satisfies $|f_i(k)|\geq\sigma$, $\forall k>T_0$, $i=1$, ..., s, and a scalar $\gamma\in(0,1)$ exists. Then, $f(k)$

can be detected by the proposed fault detection method associated with the residual $r_j(k),\ j=1,2,...,r$

$$\sigma > \frac{\left(h_{\lambda/2}\sqrt{\mathrm{Var}\{r_j(k)|H_0\}}+h_{\gamma/2}\sqrt{\mathrm{Var}\{r_j(k)|H_1\}}\right)}{\left\|\bar{I}C(I-A)^{-1}(I-A^k)F_a\right\|}. \tag{42}$$

Proof: According to (33), it can be obtained

$$\mathrm{E}\{r_j(k)|H_1\} = \mathrm{E}\{r_j(k)|H_0\} + \bar{I}C\sum_{n=0}^{k-1}A^{k-n-1}F_a f(n), \tag{43}$$

where $\bar{I}\in R^{1\times r}$, and the jth column of $\bar{I}$ is 1 and all the other columns are 0.

Denote $\Omega(f(k)) = \bar{I}C\sum_{n=0}^{k-1}A^{k-n-1}F_a f(n)$. There are two cases to be discussed as follows:

Sufficiency:

1) When $\Omega(f(k))>0$, (42) can be satisfied while $f(n)\geq\sigma, \forall k>T_f$, which means that $\exists k>T_f$

$$\Omega(f(k)) > \left(h_{\lambda/2}\sqrt{\mathrm{Var}\{r_j(k)|H_0\}}+h_{\gamma/2}\sqrt{\mathrm{Var}\{r_j(k)|H_1\}}\right).$$

Then it takes

$$\begin{aligned}
&\{k\geqslant T_f: w_j(k)\geqslant n_j(k)\}\\
&=\Big\{k\geqslant T_f: \mathrm{E}\{r_j(k)|H_1\}-h_{\gamma/2}\sqrt{\mathrm{Var}\{r_j(k)|H_1\}}\\
&\quad\geqslant \mathrm{E}\{r_j(k)|H_0\}+h_{\lambda/2}\sqrt{\mathrm{Var}\{r_j(k)|H_0\}}\Big\}\\
&=\Big\{k\geqslant T_f: \mathrm{E}\{r_j(k)|H_1\}-\mathrm{E}\{r_j(k)|H_0\}\\
&\quad\geqslant h_{\lambda/2}\sqrt{\mathrm{Var}\{r_j(k)|H_0\}}+h_{\gamma/2}\sqrt{\mathrm{Var}\{r_j(k)|H_1\}}\Big\}\\
&\supseteq\Big\{k\geqslant T_f: \Omega(f(k))>h_{\lambda/2}\sqrt{\mathrm{Var}\{r_j(k)|H_0\}}\\
&\quad+h_{\gamma/2}\sqrt{\mathrm{Var}\{r_j(k)|H_1\}}\Big\}\\
&\supseteq\left[k^*,+\infty\right).
\end{aligned}$$

So

$$\exists\hat{T}_d=\inf\{k\geqslant T_f: w(k)\geqslant n(k)\}\leqslant k^*\leqslant+\infty.$$

2) When $\Omega(f(k))<0$, (42) holds while $f(n)\leqslant-\sigma,\forall k>T_f$, which means that $\exists k>T_f$

$$\Omega(f(k)) < -\left(h_{\lambda/2}\sqrt{\mathrm{Var}\{r_j(k)|H_0\}}+h_{\gamma/2}\sqrt{\mathrm{Var}\{r_j(k)|H_1\}}\right).$$

Then it takes

$$\begin{aligned}
&\{k\geqslant T_f: z_j(k)\leqslant m_j(k)\}\\
&=\Big\{k\geqslant T_f: \mathrm{E}\{r_j(k)|H_1\}+h_{\gamma/2}\sqrt{\mathrm{Var}\{r_j(k)|H_1\}}\\
&\quad\leqslant \mathrm{E}\{r_j(k)|H_0\}-h_{\lambda/2}\sqrt{\mathrm{Var}\{r_j(k)|H_0\}}\Big\}\\
&=\Big\{k\geqslant T_f: \mathrm{E}\{r_j(k)|H_1\}-\mathrm{E}\{r_j(k)|H_0\}\\
&\quad\leqslant-\Big(h_{\lambda/2}\sqrt{\mathrm{Var}\{r_j(k)|H_0\}}\\
&\quad+h_{\gamma/2}\sqrt{\mathrm{Var}\{r_j(k)|H_1\}}\Big)\Big\}\\
&\supseteq\Big\{k\geqslant T_f: \Omega(f(k))\\
&\quad<-\Big(h_{\lambda/2}\sqrt{\mathrm{Var}\{r_j(k)|H_0\}}\\
&\quad+h_{\gamma/2}\sqrt{\mathrm{Var}\{r_j(k)|H_1\}}\Big)\Big\}\\
&\supseteq\left[k^*+\infty\right)\neq\emptyset.
\end{aligned}$$

So

$$\exists\hat{T}_d=\inf\{k\geqslant T_f: z(k)\leqslant m(k)\}\leqslant k^*\leqslant+\infty.$$

Necessity: If (42) does not hold, when $\Omega(f(k))>0$, it has

$$\begin{aligned}
0<&\Omega(f(k))\\
&<\left(h_{\lambda/2}\sqrt{\mathrm{Var}\{r_j(k)|H_0\}}+h_{\gamma/2}\sqrt{\mathrm{Var}\{r_j(k)|H_1\}}\right).
\end{aligned}$$

Then it takes

$$\begin{aligned}
&\{k\geqslant T_f: w_j(k)<n_j(k)\}\\
&=\Big\{k\geqslant T_f: \mathrm{E}\{r_j(k)|H_1\}-\mathrm{E}\{r_j(k)|H_0\}\\
&\quad<h_{\gamma/2}\sqrt{\mathrm{Var}\{r_j(k)|H_1\}}+h_{\lambda/2}\sqrt{\mathrm{Var}\{r_j(k)|H_0\}}\Big\}\\
&\supseteq\Big\{k\geqslant T_f: \Omega(f(k))\\
&\quad<h_{\lambda/2}\sqrt{\mathrm{Var}\{r_j(k)|H_0\}}+h_{\gamma/2}\sqrt{\mathrm{Var}\{r_j(k)|H_1\}}\Big\}.
\end{aligned}$$

□

Usually, the missing alarm rate $1-\chi$ is considered, it has

$$\begin{aligned}
1-\chi=&1-P(D_{test}(k)=H_1|H_1)\\
=&P(r(k)\in X(k)|H_1).
\end{aligned} \tag{44}$$

in which $D_{test}(k)$ implies the test decision at the moment k.

Therefore, if the actuator fault $f(k)$ in the hypersonic vehicle system meets detectability conditions, i.e., Theorem 2 holds, it is concluded that $\exists k^*\geqslant\hat{T}_d$

$$w(k)\geq n(k),\exists k^*\geqslant\hat{T}_d,$$

$$\chi > P(r(k) > n(k)|H_1) \geqslant P(r(k) > w(k)|H_1) = 1 - \frac{\gamma}{2}, \forall k^* \geqslant \hat{T}_d.$$

Therefore, the missing alarm rate is

$$1 - \chi < \frac{\gamma}{2}, \forall k^* \geqslant \hat{T}_d.$$

5. SIMULATION RESULT

In this section, the simulation case on a hypersonic vehicle is presented. Consider the hypersonic vehicle (10)-(12), whose parameters are introduced in Section 3. The disturbance, initial values and covariance matrices of noises are set as $d(k) = [5\sin(0.01k), 0.3\cos(0.01k)]^T$, $x(0) = x_0(0) = [8930, 0.1, 0, 0.1, 85700]$, $P(0/0) = 0.01^2 I_{5\times5}$, $Q = 0.01^2 I_{5\times5}$ and $R = 0.01^2 I_{5\times5}$, respectively.

5.1. Healthy case

For the faulty-free case, the proposed filter (15)-(20) can be used to estimate the hypersonic vehicle states V, α, q, θ and h and the wind field disturbances V_W and α_W. The estimation results are shown in Figs. 1-2, including the estimation (solid) and actual states (dashed). From Figs. 1-2, it can be seen that when the hypersonic vehicle is healthy, the proposed unknown input Kalman filter can estimate the states and disturbances of the system with the small errors, although there exist random noises in the system. Therefore, it can be known that the unknown input Kalman filter works effectively.

5.2. Faulty case

Assume that the actuator fault occurs in the hypersonic vehicle at 60s. Let the parameters $\lambda = \gamma = 0.04$ and it takes $h_{\lambda/2} = h_{\gamma/2} = 2.05$. It can be concluded that the fault can be detected when $f(k) > 0.692$ is satisfied. Here, two types of actuator faults are considered: 1) fault 1 is abrupt fault; 2) fault 2 is incipient fault.

Fault 1 (Abrupt fault):

The abrupt fault $f = [f_1, f_2]^T$ is expressed as

$$f_1 = 0,$$
$$f_2 = \begin{cases} 0, & 0\text{ s} \leqslant t < 60\text{ s}, \\ f_0, & 60\text{ s} \leqslant t \leqslant 100\text{ s}. \end{cases}$$

Let $f_0 = 0.8$, and two residual generation methods are unitized, where one is ToMFIR in (28), and another one is General Residual $r_y(k)$ in (32). The results are shown in Figs. 3 and 4. The fault detection thresholds can be obtained from the upper and lower bounds of the confidence interval $X(k)$ in (38). With $\lambda = \gamma = 0.04$, the false alarm rate of the fault is 4%. Further, Let $f_0 = 0.55$. The residuals are shown in Figs. 5 and 6.

From Fig. 3, it can be seen that the ToMFIR is within the thresholds before 60s, and exceeds the thresholds after

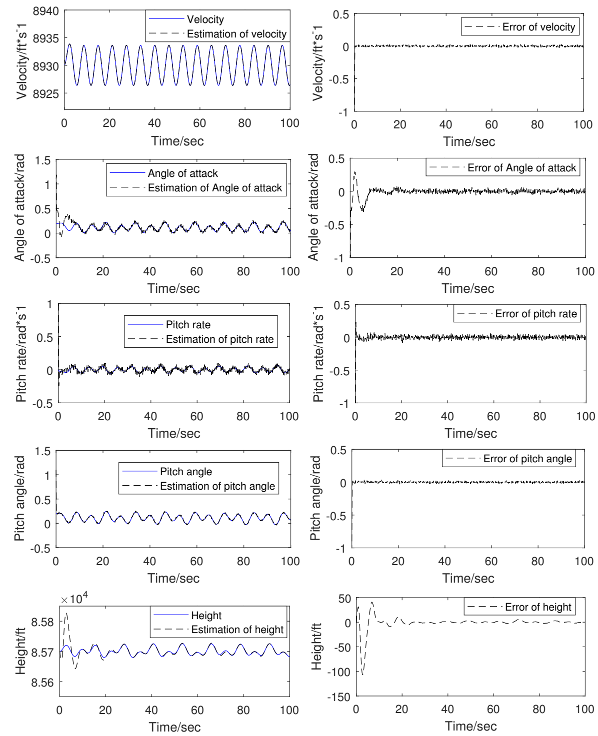

Fig. 1. State estimates (the estimate error convergence).

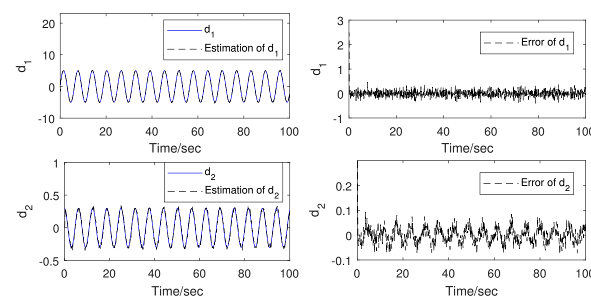

Fig. 2. Disturbance estimates (the estimate error convergence).

60 s, which shows the fault is detected effectively. But in Fig. 4, during the appearance of the fault, parts of the General Residual is still within the thresholds, which shows the fault is not detected effectively. Thus, it can be obtained that the ToMFIR is more effective for fault detection. For residuals in both Figs. 5 and 6, when fault occurs, parts of the ToMFIR and General Residual are still within the thresholds, because $f_0 = 0.55 < 0.692$ does not meet the fault detectability conditions proposed in Theorem 2.

Fault 2 (Incipient fault):

The expression of the incipient fault $f = [f_1, f_2]^T$ is chosen as

$$f_1 = 0,$$
$$f_2 = \begin{cases} 0, & 0\text{ s} \leqslant t < 60\text{ s}, \\ f_0 \times \left(1 - \mathrm{e}^{0.5\times(60-t)}\right), & 60\text{ s} \leqslant t \leqslant 100\text{ s}. \end{cases}$$

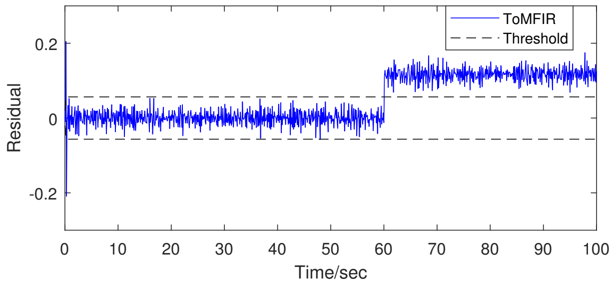

Fig. 3. Detection result of abrupt fault ($f_0 = 0.8$) by ToMFIR.

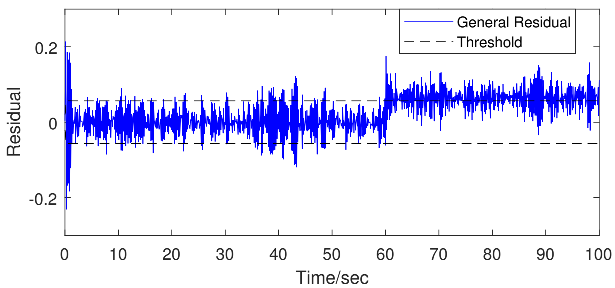

Fig. 4. Detection result of abrupt fault ($f_0 = 0.8$) by general open-loop residual.

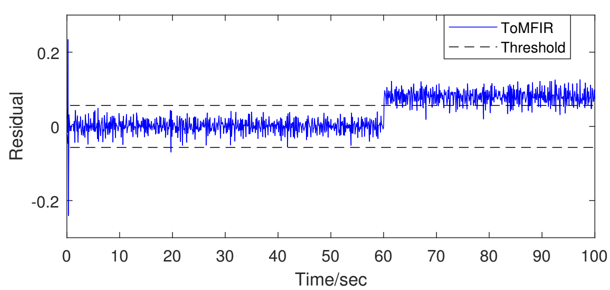

Fig. 5. Detection result of abrupt fault ($f_0 = 0.55$) by ToMFIR.

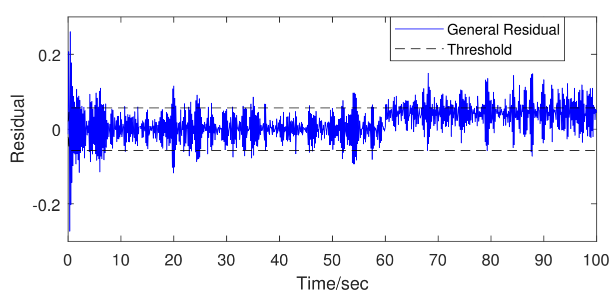

Fig. 6. Detection result of abrupt fault ($f_0 = 0.55$) by general open-loop residual.

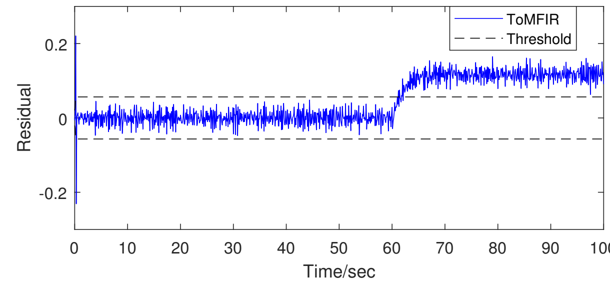

Fig. 7. Detection result of incipient fault ($f_0 = 0.8$) by ToMFIR.

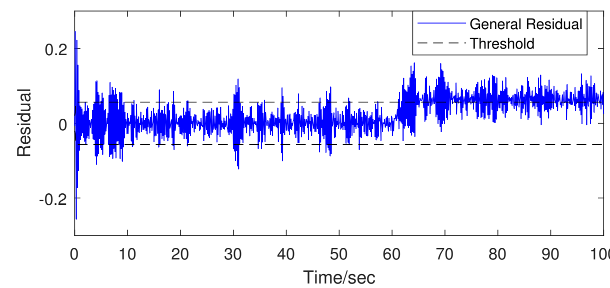

Fig. 8. Detection result of incipient fault ($f_0 = 0.8$) by general open-loop residual.

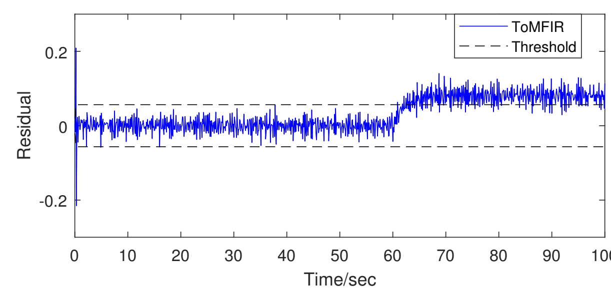

Fig. 9. Detection result of incipient fault ($f_0 = 0.55$) by ToMFIR.

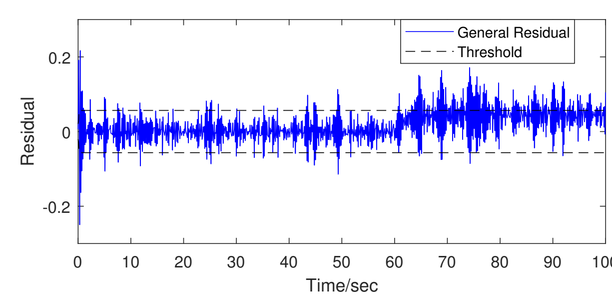

Fig. 10. Detection result of incipient fault ($f_0 = 0.55$) by general open-loop residual.

Let $f_0 = 0.8$ and 0.55, respectively, and also two residual generation methods are used as that of fault 1. The fault detection results are shown in Figs. 7-10, form which, it can be seen that the proposed ToMFIR with the fault detectability conditions can guarantee the fault be detected effectively with some detection rates.

6. CONCLUSION

In this paper, a fault detection scheme for a hypersonic vehicle closed-loop control system with actuator faults, disturbances and random noises is presented. An unknown input Kalman filter is designed to estimate the states and disturbances simultaneously, and the residual is generated by the ToMFIR method. To handle the random noises, the hypothesis test is employed to judge the ToMFIR, and the thresholds with the false alarm performance are driven. In order to obtain good detection results, the conditions for fault detection are given. Finally, the simulation verifies the effectiveness of the proposed fault detection method based on the hypothesis test. Furthermore, the proposed fault detection method will be extended to formation control, Markov switching systems [36]- [39], etc. in our future work.

REFERENCES

[1] H. X. Wu and B. Meng, "Review of research on hypersonic vehicle control," *Advances in Mechanics*, vol. 39, no. 6, pp. 756-765, 2009.

[2] P. Guan, Z. W. He, and X. S. Ge, "Neural network PID control of hypersonic vehicles," *Aerospace Control*, vol. 36, no. 1, pp. 8-13, 2018.

[3] N. M. Qi, Z. G. Song, and C. M. Qin, "Self-disturbance PID attitude control of hypersonic vehicles," *Journal of Projectiles, Missiles and Guidance*, vol. 30, no. 5, pp. 66-68, 2010.

[4] Y. Li, C. L. Wang, and Q. L. Hu, "Adaptive control with prescribed tracking performance for hypersonic flight vehicles in the presence of unknown elevator faults," *International Journal of Control*, vol. 92, no. 7, pp. 1682-1691, 2019.

[5] Z. T. Dydek, A. M. Annaswamy, and E. Lavretsky, "Adaptive control and the nasa X-15-3 flight revisited," *IEEE Control Systems*, vol. 30, no. 3, pp. 32-48, 2010.

[6] L. Fiorentini and A. Serrani, "Adaptive restricted trajectory tracking for a non-minimum phase hypersonic vehicle model," *Automatica*, vol. 48, no. 7, pp. 1248-1261, 2012.

[7] D. X. Gao and Z. Q. Sun, "Fuzzy tracking control design for hypersonic vehicles via T-S model," *Science in China, Series F (Information Science)*, vol. 54, no. 3, pp. 521-528, 2011.

[8] G. Wu and X. Meng, "Nonlinear disturbance observer based robust backstepping control for a flexible air-breathing hypersonic vehicle," *Aerospace Science and Technology*, vol. 54, no. 1, pp. 174-182, 2016.

[9] J. G. Sun, S. M. Song, H. T. Chen, and G. Q. Wu, "Fast terminal sliding mode tracking control of hypersonic vehicles based on non-homogeneous disturbance observer," *International Journal of Control, Automation, and Systems*, vol. 15, no. 6, pp. 2646-2659, 2017.

[10] W. Tang, W. Long, and H. Gao, "Model predictive control of hypersonic vehicles accommodating constraints," *IET Control Theory and Applications*, vol. 11, no. 15, pp. 2599-2606, 2017.

[11] S. Liu, B. Jiang, Z. Mao, and S. X. Ding, "Adaptive backstepping based fault-tolerant control for high-speed trains with actuator faults," *International Journal of Control, Automation and Systems*, vol. 17, no. 6, pp. 1408-1420, 2019.

[12] P. Apkarian and R. J. Adams, "Advanced gain-scheduling techniques for uncertain systems," *IEEE Transactions on Control Systems Technology*, vol. 6, no. 1, pp. 21-32, 1998.

[13] J. Jiang, "Design of reconfigurable control systems using eigenstructure assignments," *International Journal of Control*, vol. 59, no. 2, pp. 395-410, 1994.

[14] C. H. Jing, H. G. Xu, and X. J. Niu, "Adaptive sliding mode disturbance rejection control with prescribed performance for robotic manipulators," *ISA Transactions*, vol. 91, no. 1, pp. 41-51, 2019.

[15] H. Zhang, R. R. Wang and J. M. Wang, "Robust finite frequency $H\infty$ passive fault tolerant static output feedback control with application to active vibration attenuation," *IFAC Proceedings Volumes*, vol. 46, no. 5, pp. 340-346, 2013.

[16] J. Yu and M. Chen, "Fault tolerant control for near space vehicles with input saturation using disturbance observer and neural networks," *Circuits, Systems, and Signal Processing*, vol. 34, no. 7, pp. 2091-2107, 2015.

[17] Q. Shen, B. Jiang, and V. Cocquempot, "Fault-tolerant control for T-S fuzzy systems with application to near-space hypersonic vehicle with actuator faults," *IEEE Transactions on Fuzzy Systems*, vol. 20, no. 4, pp. 652-665, 2012.

[18] C. F. Hu, X. F. Wei, and Y. L. Ren, "Passive fault-tolerant control based on weighted LPV tube-MPC for air-breathing hypersonic vehicles," *International Journal of Control, Automation, and Systems*, vol. 17, no. 8, pp. 1957-1970, 2019.

[19] Y. F. Xu, B. Jiang, and R. Y. Qi, "Near-space vehicle fault diagnosis and fault-tolerant control based on fuzzy T-S adaptive observer," *Journal of Southeast University (Natural Science Edition)*, vol. 39, no. S1, pp. 189-194, 2009.

[20] X. Cai and F. Wu, "Multiobjective fault detection and isolation for flexible air-breathing hypersonic vehicle," *Journal of Systems Engineering and Electronics*, vol. 22, no. 1, pp. 52-62, 2011.

[21] E. R. Abraham, G. Ivan, and J. G. Rangel-Peraza, "Wind-gust compensation algorithm based on high-gain residual observer to control a quadrotor aircraft: real-time verification task at fixed point," *International Journal of Control Automation and Systems*, vol. 16, no. 6, pp. 856-866, 2018.

[22] S. H. S. Ziyabari and M. A. Shoorehdeli, "Robust fault diagnosis scheme in a class of nonlinear system based on UIO and fuzzy residual," *International Journal of Control, Automation and Systems*, vol. 15, no. 3, pp. 1145-1154, 2017.

[23] M. N. Piao, Z. H. Yang, M. W. Sun, J. Huang, and Z. Q. Chen, "A practical attitude control scheme for hypersonic vehicle based on disturbance observer," *Proceedings of the Institution of Mechanical Engineers*, vol. 233 no. 12. pp. 4523-4540, 2019.

[24] Y. Fan, W. X. Zhu, and G. Z. Bai, "A cost-effective tracking algorithm for hypersonic glide vehicle maneuver based on modified aerodynamic model," *Applied Sciences*, vol. 6, no. 10, pp. 312-328, 2016.

[25] J. J. He, R. Y. Qi, B. Jiang, and R. Y. Zhai, "Fault-tolerant control with mixed aerodynamic surfaces and RCS jets for hypersonic reentry vehicles," *Chinese Journal of Aeronautics*, vol. 30, no. 2, pp. 780-795, 2017.

[26] Q. Wang and R. F. Stengel, "Robust nonlinear control of a hypersonic aircraft," *Journal of Guidance, Control, and Dynamics*, vol. 23, no. 4, pp. 577-585, 2000.

[27] H. J. Xu, M. D. Mirmirani, and P. A. Ioannou, "Adaptive sliding mode control design for a hypersonic flying vehicle," *Journal of Guidance, Control and Dynamics*, vol. 27, no. 5, pp. 829-838, 2004.

[28] Y. M. Chen, Y. L. He, and M. F. Zhou, "Decentralized PID neural network control for a quadrotor helicopter subjected to wind disturbance," *Journal of Central South University of Technology*, vol. 22, no. 1, pp. 168-179, 2015.

[29] L. Y. Wen, G. Tao, H. Yang, and B. Jiang, "Aircraft turbulence compensation using adaptive multivariable disturbance rejection techniques," *Journal of Guidance, Control, and Dynamics*, vol. 38, no. 5, pp. 954-963, 2015.

[30] J. Chen and R. J. Patton, *Robust Model-based Fault Diagnosis for Dynamic Systems*, Springer, US, 1999.

[31] M. Darouach, M. Zasadzinski, A. Bossong-Onna, and S. Nowakowski, "Kalman filtering with unknown inputs via optimal state estimation of singular systems," *International Journal of Systems Science*, vol. 26, no. 10, pp. 2015-2028, 1995.

[32] P. K. Kitanidis, "Unbiased minimum-variance linear state estimation," *Automatica*, vol. 23, no. 6, pp. 775-778, 1987.

[33] C. K. Chui and G. R. Chen, *Kalman Filtering with Real-time Applications*, Springer-Verlag, 1987.

[34] S. Y. Wang, *Principles of Nonlinear Kalman Filters and Their Applications*, Electronic Industry Press, 2015.

[35] F. N. Chowdhury, "Fault detection in closed loop adaptive systems," *Proc. of IEEE Mountain Workshop on Adaptive and Learning Systems (SMCals 2006)*, pp. 160-164, 2006.

[36] J. Cheng, J. H. Park, X. D. Zhao, H. Karimi, and J. D. Cao, "Quantized nonstationary filtering of network-based Markov switching RSNSs: a multiple hierarchical structure strategy," *IEEE Transactions on Automatic Control*, 2019. DOI: 10.1109/TAC.2019.2958824

[37] J. Cheng, D. Zhang, W. Qi, J. Cao, and K. Shi, "Finite-time stabilization of T-S fuzzy semi-Markov switching systems: A coupling memory sampled-data control approach," *Journal of the Franklin Institute*, 2019. DOI: 10.1016/j.jfranklin.2019.06.021

[38] J. Cheng and Z, Yang, "Nonstationary l_2-l_∞ filtering for Markov switching repeated scalar nonlinear systems with randomly occurring nonlinearities," *Applied Mathematics and Computation*, vol. 365, 124714, 2020.

[39] J. Cheng, J. H. Park, X. D. Zhao, J. Cao, and W. Qi, "Static output feedback control of switched systems with quantization: A nonhomogeneous sojourn probability approach," *International Journal of Robust and Nonlinear Control*, vol. 29, no. 17, pp. 5992-6005, 2019.

Xunhong Lv obtained her Ph.D. degree in the College of Automation Engineering, Nanjing University of Aeronautics and Astronautics. Her research interests are fault tolerant flight control, system identification and fault tolerant flight control computer system.

Yifan Fang received her B.S. degree in automation engineering from Nanjing University of Aeronautics and Astronautics, China, in 2017. She is currently pursuing a Master's degree from the College of Automation Engineering in Nanjing University of Aeronautics and Astronautics, Nanjing, China. Her current research interests include adaptive fault-tolerant control and its applications.

Zehui Mao received her Ph.D. degree in control theory and control engineering from Nanjing University of Aeronautics and Astronautics, Nanjing, China, in 2009. She is now a professor at the College of Automation Engineering in Nanjing University of Aeronautics and Astronautics, China. She has won the Outstanding Youth Science Foundation Project. She worked in the areas of fault diagnosis, with particular interests in nonlinear control systems, sampled-data systems and networked control systems. Her current research interests include fault diagnosis and fault-tolerant control of systems with disturbance and incipient faults, and high speed train and spacecraft flight control applications.

Bin Jiang received his Ph.D. degree in automatic control from Northeastern University, Shenyang, China, in 1995. He had ever been a Post-Doctoral Fellow, a Research Fellow, an Invited Professor, and a Visiting Professor in Singapore, France, USA, and Canada, respectively. He is currently a Chair Professor of Cheung Kong Scholar Program with the Ministry of Education and the Vice President of Nanjing University of Aeronautics and Astronautics, Nanjing, China. He won the second class Prize of National Natural Science Award of China. He is a Fellow of Institute of Electrical and Electronics Engineers (IEEE), and also a Fellow of Chinese Association of Automation (CAA). He currently serves as an Associate Editor or an Editorial Board Member for a number of journals, such as the IEEE Trans. On Cybernetics, Journal of the Franklin Institute, Neurocomputing at. He is a Chair of Control Systems Chapter in IEEE Nanjing Section, a member of IFAC Technical Committee on Fault Detection, Supervision, and Safety of Technical Processes. His research interests include fault diagnosis and fault tolerant control and their applications in aircrafts, satellites and high-speed trains.

Ruiyun Qi received her B.E. degree in automatic control from University of Science and Technology of China in 2001, and a Ph.D. degree in electrical engineering from University of Birmingham, UK, in 2007. She joined the College of Automation Engineering, Nanjing University of Aeronautics and Astronautics, in 2008. Now she is a professor. Her research interests include fuzzy adaptive control, fault-tolerant control and their applications.